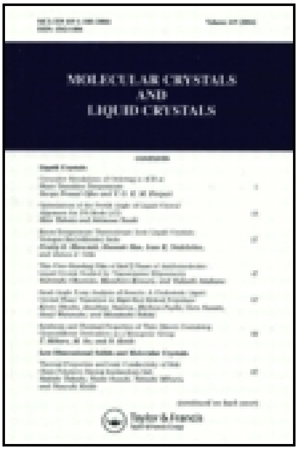

Molecular Crystals and Liquid Crystals

Publication details, including instructions for authors and subscription information:
http://www.tandfonline.com/loi/gmcl16

Application and Device Modeling of Liquid Crystal Displays

Tatsuo Uchida [a]

[a] Department of Electronic Engineering Faculty of Engineering, Tohoku University, Sendai, 980, Japan

Version of record first published: 17 Oct 2011.

To cite this article: Tatsuo Uchida (1985): Application and Device Modeling of Liquid Crystal Displays, Molecular Crystals and Liquid Crystals, 123:1, 15-55

To link to this article: http://dx.doi.org/10.1080/00268948508074766

Mol. Cryst. Liq. Cryst., 1985, Vol. 123, pp. 15–55
0026-8941/85/1234-00015/$30.00/0

Application and Device Modeling of Liquid Crystal Displays

TATSUO UCHIDA

Department of Electronic Engineering Faculty of Engineering, Tohoku University Sendai, 980 Japan

(*Received September 17, 1984*)

Many kinds of modes of liquid crystal display have been considered by using various types of liquid crystals, their surface alignments and optical effects. Among these modes, the twisted nematic mode (TN-mode) is most widely used, so that fundamental device modeling of this type display is discussed on surface treatments of substrates, and on design condition of material and device parameters.

The next trend of development of the liquid crystal displays are increasing information contents, realization of multicolor or full-color display, increasing the display size and improvement of response speed. Their prospects and problems are also discussed.

1. INTRODUCTION

Liquid crystal was discovered by Reinitzer in 1888, about 100 years ago, but it is just recently that application of liquid crystal has been positively considered. It started by Fergason[1] by using cholesteric liquid crystal in the middle of 1960's, but it is well known that great interest was focussed on the liquid crystal in the engineering field after Heilmeier, et al.[2] reported about dynamic scattering in 1968.

Around these years, semiconductor technology had been progressing, and accordingly display devices were required to progress from simple indicators to more complicated displays such as numeric displays. Since then, competition of liquid crystal displays with emissive displays such as Nixie tubes, light emitting diodes, vacuum fluorescent displays has started.

Until this time, Organic and besides liquid material had almost never used as an active material of electronic devices. Moreover, display quality of the liquid crystal display was relatively poor by comparison with the emissive displays, so that it was very difficult for the liquid crystal displays to be accepted as a display devices. But fortunately, the energy saving conscious has risen since 1975. On the other hand, complimentary MOS technology had developed and power consumption of driver decreased very much. This driver was combined with the liquid crystal displays and new products such as handy electric calculators and digital watches were realized. Such success of the practical application of the LC display was much indebted to development of various materials and technology as follows:

- Liquid crystal material
- Indium tin oxide electrode
- Flat, soda-lime glass plate
- Protection layer for alkali ion
- Molecular orientation layer
- Gap control technique
- Perimeter seal resin
- End seal Technology
- Interconnection between liquid crystal display and driver circuits
- Polarizer
- CMOS-driver

As shown here, the liquid crystal display is based on various technology concerning chemistry, physics and electronic engineering, while in this paper the author will focus the discussion on the liquid crystal device itself.

2. SURFACE ALIGNMENT

In the liquid crystal devices, one of the most important problems is the surface alignment of the liquid crystal molecules. There are four basic surface alignments as shown in Figure 1. In practical application, a small tilt from parallel and perpendicular as shown in figures (c) and (d), namely, pretilt is important for obtaining domain-free orientation under electric field. However, let us consider these tilted alignments to be included into parallel or perpendicular alignments for simplification, if not mentioned especially.

Mechanism and method to obtain stable surface alignment have been studied by many researchers. One concise theory on mechanism of the surface alignment is Creagh's,[3] Kahn's[4] and Porte's[5] one, which is based on the relation between surface energies of the substrate and

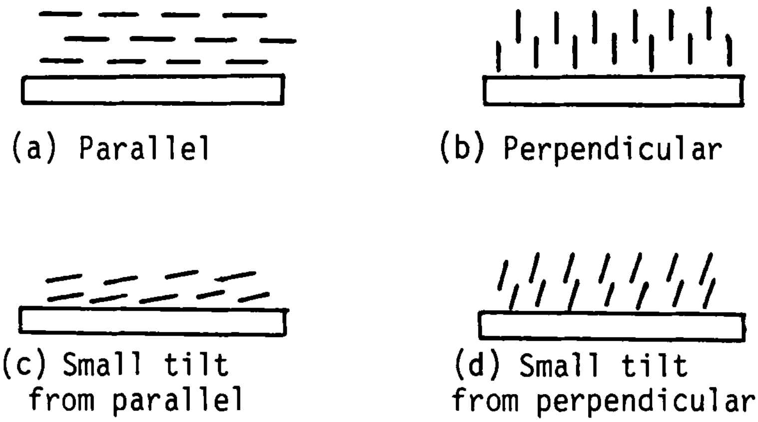

FIGURE 1 Fundamental molecular alignments on substrate surfaces.

liquid crystal, while several experimental results contradicting their theory[6,7] have also been reported. Explanation of the mechanism on the surface alignment has not yet been established but the authors have an idea of the alignment that there are three mechanisms of the perpendicular alignment as shown in Figure 2. The first one is the amphiphilic material assisted alignment as shown in figure (a).[8,9] That is, amphiphilic material absorbs perpendicularly to the polar surface and liquid crystal aligns according to the amphiphilic material. This amphiphilic material is sometimes an impurity contained in the liquid crystal or surfactant. Surfactants reported by Haller,[10] Helfrich[11] and Proust, et al.[12] correspond to this kind of amphiphilic material. As for the surface polarity, the author, et al.[8,9] have evaluated the polarity of various surfaces by using liquid crystal chromatographic effect. The result is shown in Table I. It is seen from this table that

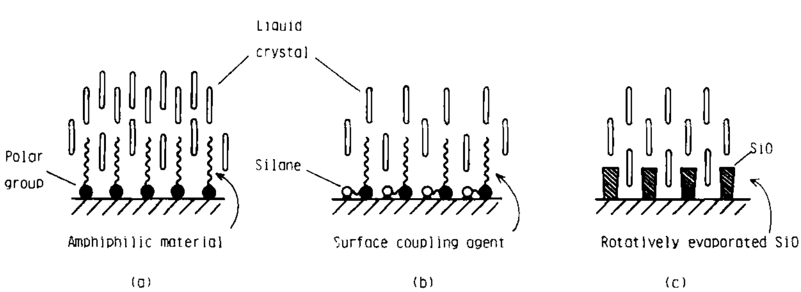

FIGURE 2 Mechanisms of the perpendicular alignment for surface with strong polarity (a), for surface treated with surface coupling agents (b), and for SiO-rotatively evaporated surface (c).

surfaces with strong polarity have tendency of the perpendicular alignment for liquid crystals with amphiphilic impurity (MBBA and 7CB). The second mechanism is the perpendicular alignment obtained by surface coupling agent as shown in Figure 2 (b). This material is usually silanes with long alkyl chain as reported by Kahn[4] and many other workers.[6,7,13,14] The third mechanism is microscopic columnar structure-assisted alignment as shown in Figure 2(c). This kind of surface is obtained by SiO-rotatively oblique evaporation as reported by Hiroshima, et al.[15]

TABLE I

Polarity of various surfaces and liquid crystal orientation on them (MBBA and 7CB contain small amount of amphiphilic impurities)[9]

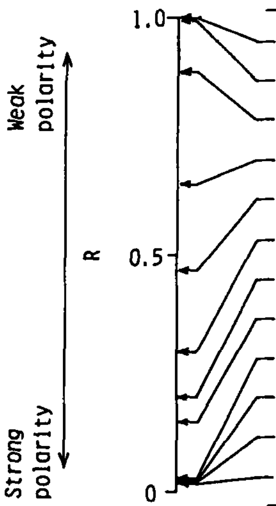

Oxide material	Liquid crystal orientation		
	BAB	MBBA	7CB
Au	$\parallel$	($\parallel$)	($\parallel$)
CeO_2	$\parallel$	($\parallel$)	($\parallel$)
WO_3	$\parallel$	($\parallel$)	($\parallel$)
SiO_2	$\parallel$	($\parallel$)	($\parallel$)
Soda-glass	$\parallel$	($\parallel$)	($\parallel$)
SnO_2	$\parallel$	($\parallel$)	
ZrO_2	$\parallel$	$\perp$	$\perp$
Heated-glass	$\parallel$	$\perp$	$\perp$
In_2O_3	$\parallel$	$\perp$	$\perp$
Al_2O_3	$\parallel$	$\perp$	$\perp$
Al	$\parallel$	$\perp$	$\perp$
MgO	$\parallel$	$\perp$	$\perp$

R : Reduced length of adsorption area of an impurity in the liquid crystal chromatography

$\perp$: Homeotropic, $\parallel$: Parallel
($\parallel$) : Nearly parallel, • : Undistinguish

BAB : p,p'-di(n-butyl)-azoxybenzene
MBBA : p-methoxybenzylidene-p'-n-butylaniline
7CB : p-n-heptyl-p'-cyanobiphenyl

According to the Creagh and other's theory as mentioned above, homeotropic alignment is induced on the low energy surface. This fact itself is true because almost all surfaces of homeotropic treatment by surfactants or surface coupling agents have perpendicularly aligned alkyl chain or fuluorocarbon chain as shown in Table II, and this kind of surface has clearly low energy. But we confirmed that the reverse is not necessary true, for example, a teflon-evaporated and rubbed surface induces the parallel alignment though its surface energy is low.

Parallel alignment is usually obtained as long as the surface is microscopically flat and liquid crystal does not contain amphiphilic impurity or surface polarity is too low to adsorb the impurity.[8,9]

TABLE II

Surface structures which were reported to have low surface energy[7]

Worker	Surface	Surface structure
Creagh et al.[3]	lecithin treated surface	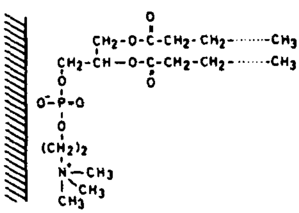
	hexadecyltrimethyl-ammonium bromide treated surface	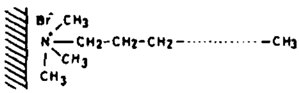
Funada et al.[16]	N,N-dimethyl-N-octadecyl-3-aminopropyltrimethoxy-silyl chloride (DMOAP) treated surface	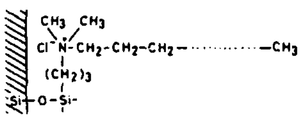
	N-perfluoroctylsulphonyl-3-aminopropyltrimethyl-ammonium iodide treated surface	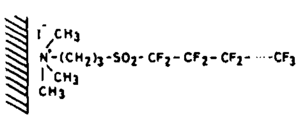
Porte[5]	alkylmonoamine treated surface	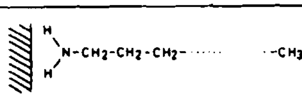

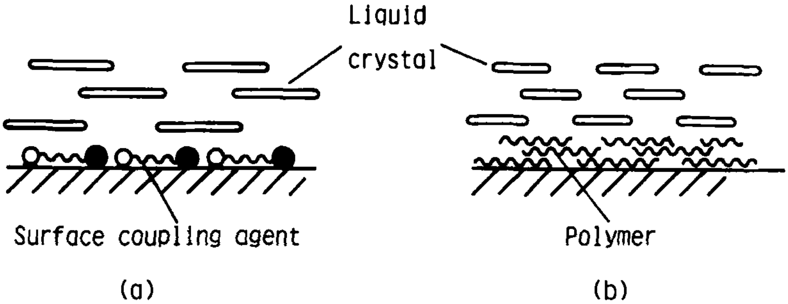

FIGURE 3 Mechanisms of the parallel alignment for surfaces treated with surface coupling agent (a), and coated with polymers (b).

Therefore, stable parallel alignment is obtained by decreasing the surface polarity by coating polymer[17,18] or surface coupling agent,[4,7,13,17] of which molecules tend to adsorve parallel to the surface as shown in Figure 3. However, these alignment are random parallel alignment. In order to obtain homogeneous alignment, unidirectional rubbing is necessary. Mechanism of the alignment parallel to the rubbing direction is analyzed by Berreman.[19] He estimated the difference of elastic energies between parallel and perpendicular alignments to the grooves to be about 4×10^5 erg/cm^3 for the surface rubbed with diamond paste. But for the usual rubbed surface with cloth, the grooves are not observed even by the electron microscope. Therefore the mechanism of the homogeneous alignment of the usual rubbed surface might not grooves but is considered to be due to statistically parallel alignment of some impurities coated by rubbing or surface molecules of orientation layer.

An interesting fact of the rubbed surface is that small tilt alignment is obtained. The angle is around 0.5° to 3°, which is important in liquid crystal display as mentioned before, while the mechanism has not yet clarified. The author considers that the tilt alignment is due to the surface structure as shown in Figure 4(a), or due to tails of organic impurities or organic material of the orientation layer as shown in Figure 4(b). Tilted alignment is also obtained by oblique evaporation of SiO or some other inorganic materials as reported by Junning.[20] The surface structure as shown in Figure 5(a) and liquid crystal alignment is analyzed by Goodman.[21] Combination of the oblique evaporation and the perpendicular surface coupling agent as shown in Figure 5(b) is also studied,[22] and small tilt alignment from

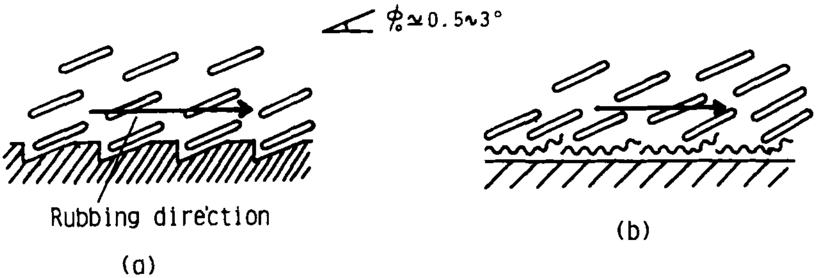

FIGURE 4 Conceivable mechanisms of the tilted homogeneous alignment on rubbed surface.

perpendicular to the surface was obtained. The tilted angle is arbitrarily controlled between 0° to about 30° by evaporation condition.

In the nematic liquid crystal cells, there are fundamentally four combinations of the surface alignments mentioned previously. Those are as shown in Figure 6 where tilted alignment is neglected for simplification. As for the cholesteric liquid crystal cells, there are three fundamental alignments as shown in Figure 7, where figure (a) corresponds to the parallel surface alignment and figure (b) corresponds to the perpendicular surface alignment. Figure 8 shows the fundamental alignments of the smectic liquid crystals.

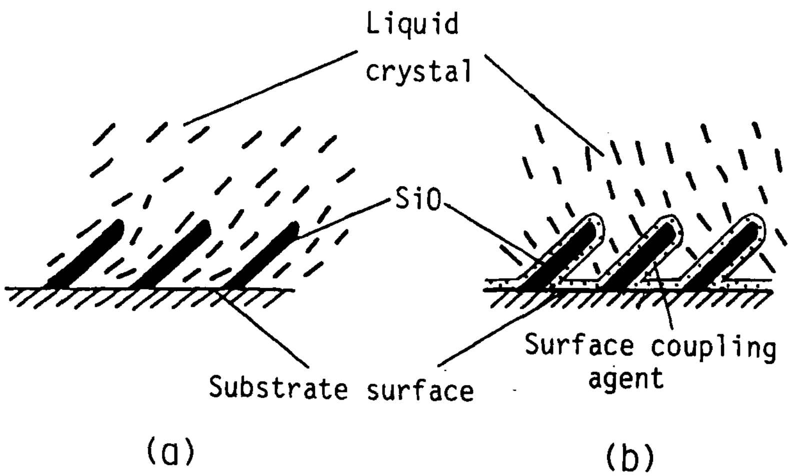

FIGURE 5 Mechanisms of liquid crystal orientation for SiO-obliquely evaporated surfaces without (a)[21] and with (b) the perpendicular surface coupling agent.

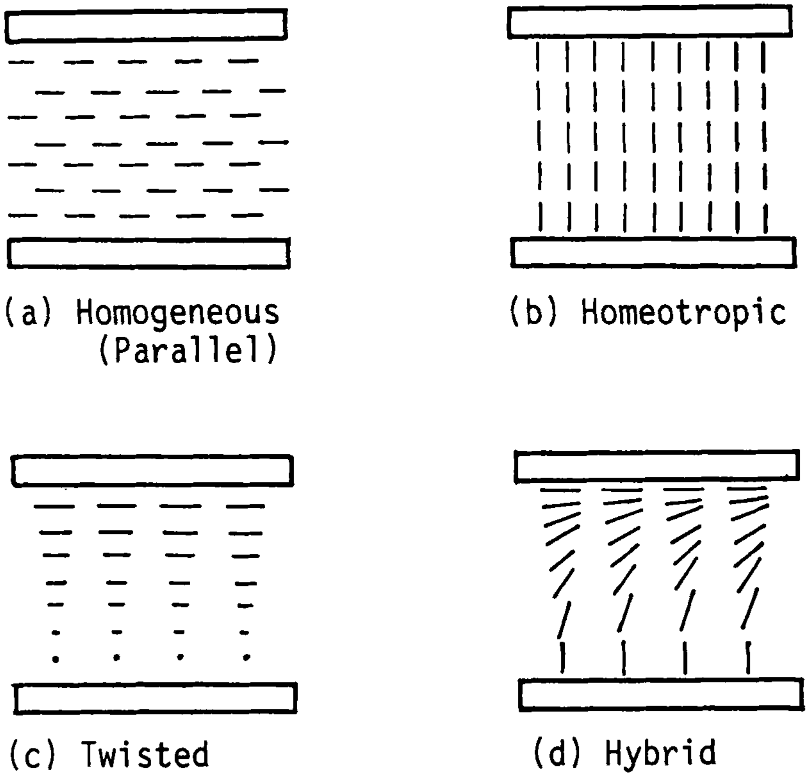

FIGURE 6 Fundamental molecular alignments of the nematic liquid crystal cell.

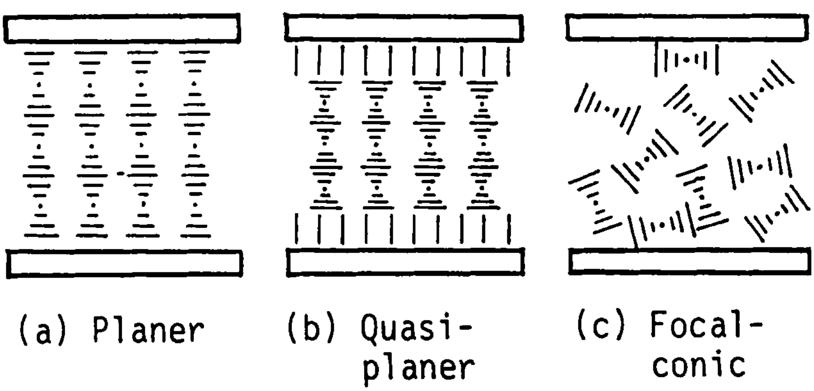

FIGURE 7 Fundamental molecular alignments of the cholesteric liquid crystal cell.

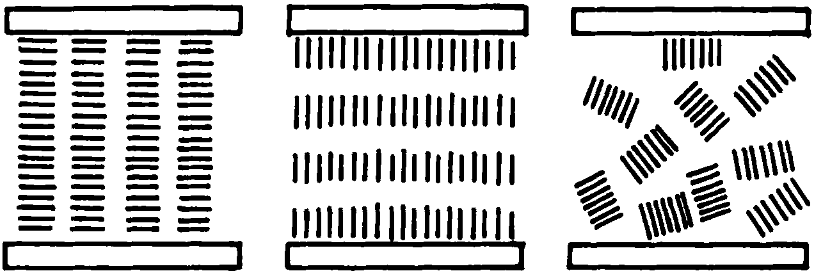

FIGURE 8 Fundamental molecular alignments of the smectic liquid crystal cell.

3. VARIOUS MODES OF THE LIQUID CRYSTAL DISPLAY

Applicable optical effects to liquid crystal displays are

- Birefringence
- Rotation of polarized direction
- Absorption
- Diffraction

Combining various molecular alignments mentioned previously, various types of liquid crystal and optical effects, variety of liquid crystal displays can be considered. Table III–VI show liquid crystal molecular alignments at off- and on-states, threshold voltage V_{th} and the display modes for nematic and cholesteric liquid crystals with positive and negative dielectric anisotropy ($\Delta\epsilon$). Among many liquid crystal modes mentioned in these tables, the twisted nematic mode (TN-mode) is most widely used. The reasons why this type cell is widely used are relatively wide viewing angle, high contrast, low driving voltage and low current and good multiplexibility because of sharp threshold. Therefore, the device modeling of this type cell is discussed in detail in the next section.

4. TWISTED NEMATIC LIQUID CRYSTAL CELL (TN-CELL)

For the first, TN-cell require stable parallel surface alignment. As mentioned before, in order to obtain stable parallel alignment, the

TABLE III

Display modes of nematic liquid crystal with positive dielectric anisotropy

No	Alignment off	Alignment on	V_{th}	Display modes
1			~1V	ECB[23], GH[24]
2			~1V	ECB[25], TN[26], GH[27]
3			-	ECB[28]

ECB : Electrically controled birefringence mode
TN : Twisted nematic mode
GH : Guest-host mode

TABLE IV

Display modes of nematic liquid crystal with negative $\Delta\epsilon$

No	Alignment off	Alignment on	V_{th}	Display modes
1	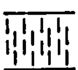		~1V (high frequency)	ECB[29,30], GH[31]
2		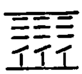	- (high frequency)	ECB[28,32]
3			~7V (low frequency)	DS
4	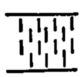		~7V (low frequency)	DS
5			~7V (low frequency)	DS, DTN[33,34]

DS : Dynamic scattering mode
DTN : Depolarization in a twisted nematic mode

TABLE V

Display modes of cholesteric liquid crystal with positive $\Delta\epsilon$

No	Alignment off	Alignment on	V_{th}	Display mode
1		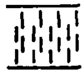	10V*)	PC [35]
2	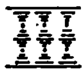	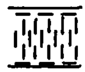	~2V*)	GH(WT) of long P [36]
3	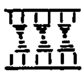	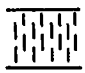	5~10V*)	GH(WT) of short P [36]
4	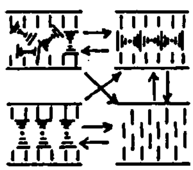		~2V*) 10~20V*)	Memory [37]

PC : Cholesteric nematic phase change
GH(WT) : White-Taylor type GH-mode
(P : Helical pitch)
*) Depend on cell thickness and helical pitch

surface polarity must be decreased to avoid adsorption of impurities.[11,12] Unfortunately indium tin oxide electrode and heat treated soda-lime glass substrate have strong polarity as shown in Table I. The strong polarity of the soda-lime glass is confirmed to be due to sodium ion.[9] These surface must be covered by materials of weak polarity such as silicon dioxide or some organic material. Therefore, the glass substrate of the liquid crystal display is usually covered by silicon dioxide layer of 1000 ~ 2000 Å to protect migration of the sodium ion from bulk to the surface as shown in Figure 9. Top of the substrate are covered by orientation layer such as polyimid.

TABLE VI

Display modes of cholesteric liquid crystal with negative $\Delta\epsilon$

No	Alignment off	Alignment on	V_{th}		Display mode
1	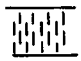	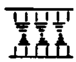	∿ 1V		PC-GH[38]
2	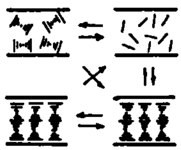		10V*)	low frequency	Memory[39]
			10∿20V*)	high frequency	

PC-GH : Phase change type GH with positive image display

*) Depend on cell thickness and helical pitch

Another important condition we should note in fabrication of the twisted nematic cell is matching of the twist sense and rubbing direction or pretilt-direction. There are four combinations of them as shown in Figure 10. Two cases of them are splay alignment and hence reverse tilt domains are appeared when voltage is applied. The non-splay alignment as shown in Figure (a) or (d) is applicable in actual cell. The twist sence is controlled by doping with small amount of chiral material such as cholesteric liquid crystal or optically active material.

Also, important factor concerning the display quality of the TN-cell is the product of birefringence and cell gap, Δnd. Figure 11 shows

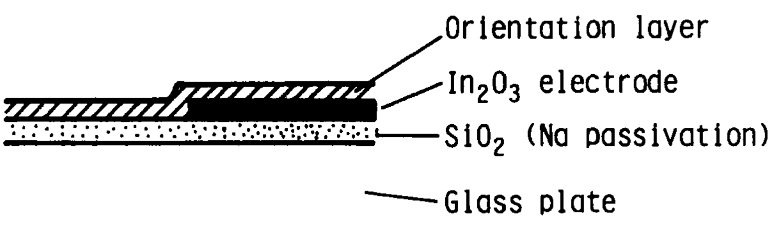

FIGURE 9 Glass substrate of the liquid crystal display.

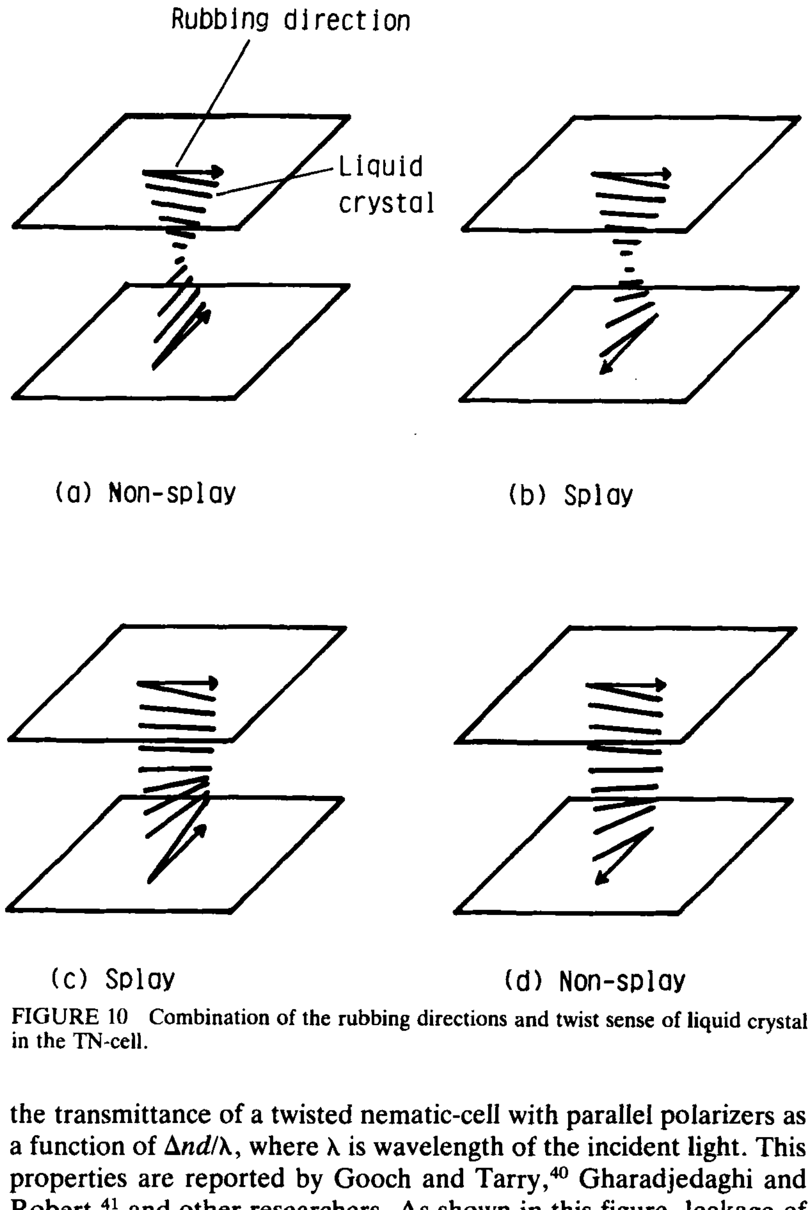

FIGURE 10 Combination of the rubbing directions and twist sense of liquid crystal in the TN-cell.

the transmittance of a twisted nematic-cell with parallel polarizers as a function of $\Delta nd/\lambda$, where λ is wavelength of the incident light. This properties are reported by Gooch and Tarry,[40] Gharadjedaghi and Robert,[41] and other researchers. As shown in this figure, leakage of transmittance increases gradually and interference color is appeared when $\Delta nd/\lambda$ decreased smaller than about 2. Therefore, $\Delta nd/\lambda$ is adjusted around 2 in the usual twisted nematic cells. Pohl, et al.,[42] however, proposed recently that the cell with Δnd of around 0.5 μm

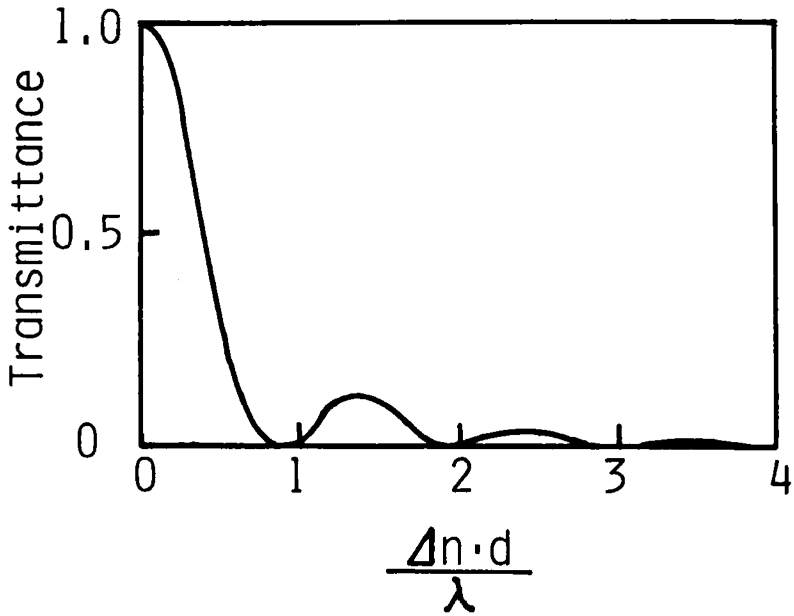

FIGURE 11 Transmittance of the TN-cell with parallel polarizers as a function of $\Delta n \cdot d/\lambda$.

which correspond to $\Delta nd/\lambda$ of about 0.9, have small leakage and wide viewing angle. The authors tried to calculate the contrast ratio of the twisted nematic cell defined by the ratio of luminous transmittances $T_{\ell m}$ at on- and off-states as follows:

$$\text{Contrast ratio} = \frac{T_{\ell m}\,(\text{on})}{T_{\ell m}\,(\text{off})} = \frac{\int T_{on}(\lambda)\cdot \nu(\lambda)d\lambda}{\int T_{off}(\lambda)\cdot \nu(\lambda)d\lambda},$$

where $\nu(\lambda)$ is relative luminous efficiency. The result is shown in Figure 12. It is seen that Δnd of about 0.5 μm gives higher contrast than usual condition of 1.1 μm but it is very narrow peak and hence high accuracy of cell-gap over whole area of the cell is required.

In addition to the transmissive problem, these is interference colored problem caused by the same mechanism. Figure 13 shows the typical interference color for the TN-cell with crossed polarizers in the 1931 CIE chromaticity diagram as a function of Δnd, where "W" indicates the white point and distance from this point corresponds to the strength of the coloration, and its azimuth indicates hue. From this figure, interference color does not change when $\Delta nd \gtrsim 1.0$ μm,

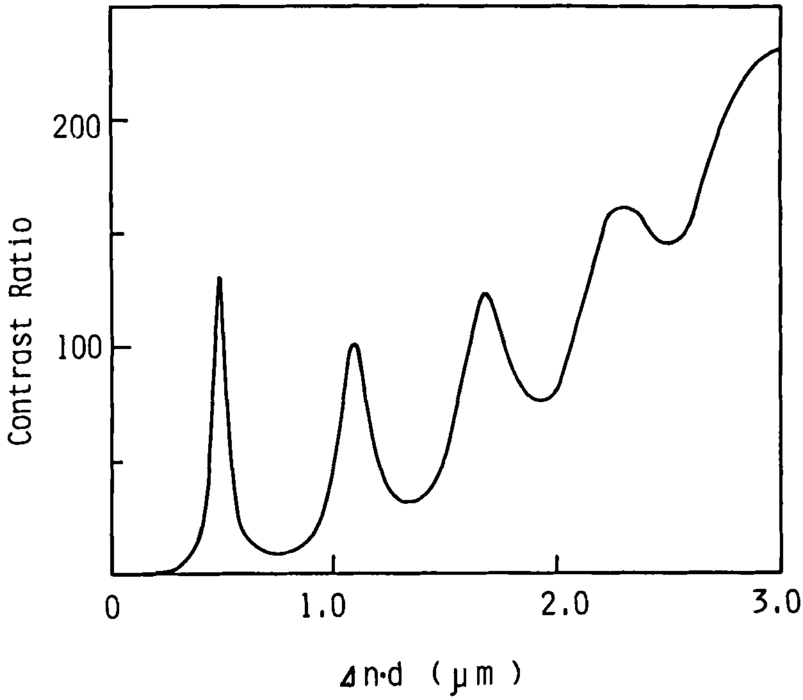

FIGURE 12 Luminous contrast of the TN-cell as a function of $\Delta n{\cdot}d$.

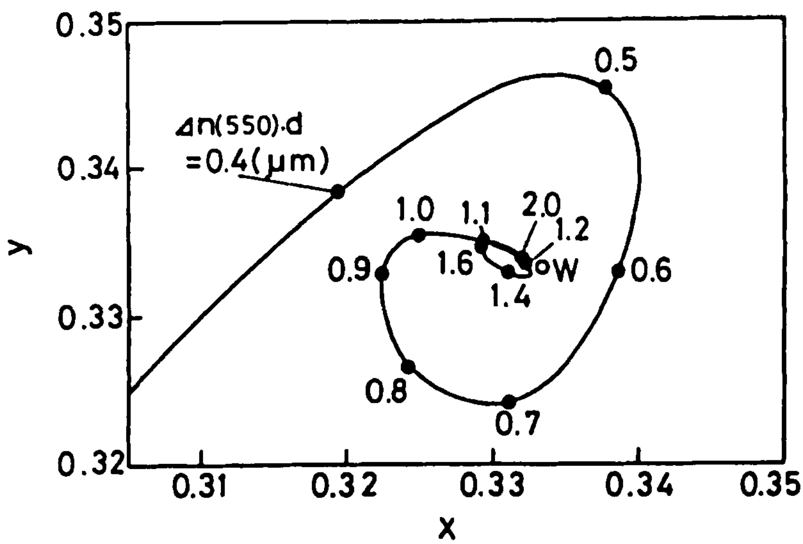

FIGURE 13 A locus of interfarence color of a TN-cell with a Shiff-base mixture and crossed polarizers as a function of Δn (550) d on the 1931 CIE chromaticity diagram.

while it changes sensitively around 0.5 μm. Therefore, also from this point of view, Pohl's condition requires high accuracy of cell-gap control.

As for the liquid crystal material for the twisted nematic liquid crystal display, Shiff base mixture as No. 1 in Table VII was used at early time, but it is well known to be unstable to moisture. Azoxy compound was also used, but it was unstable to light. In 1973, Cyanobiphenyl as No. 2 was synthesized by Gray, et al.[43] and this material was found to be chemically, electrochemically and photochemically stable. This material contributed very much to liquid crystal display in removing the frit seal and simplifying the production process. Then, liquid crystal materials or additives for increasing clearing temperature T_{NI} and dielectric anisotropy $\Delta\epsilon$, and decreasing crystallization temperature T_{CN}, viscosity η and birefringence Δn as No. 3 to 14 have been synthesized one after another. In present liquid crystal displays, a mixture of several compounds as shown in Table VII is used according to purpous and required characteristics.

5. TRENDS OF THE DEVELOPMENT OF THE LIQUID CRYSTAL DISPLAYS

Based on the material- and device-chemistry, physics and technology, the liquid crystal displays of the first generation have been most widely used in the field of small numeric displays. The next trends of the development of the liquid crystal displays are

- Display with large information contents
- Color display
- Large screen
- High speed

These items are discussed in the following sections.

5.1 Display with large information contents

5.1.1 Direct matrix display

Direct matrix liquid crystal display is driven by line at a time method. Namely, X-electrodes are scanned one by one, and data signals are simultaneously applied to Y-electrodes. This system was well analyzed by Alt and Pleshko.[44] In this case, the ratio of effective voltage applied to on- and off-pixels is given as a function of scanning line

TABLE VII

Liquid crystal materials for the TN-cell

	Liquid crystal	Feature
No.1	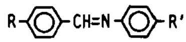 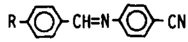	
No.2	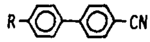	Stable
No.3	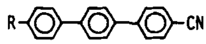	Increase T_{NI}
No.4	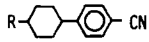	Decrease η, Δn and T_{CN}
No.5	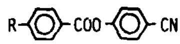	Increase $\Delta\varepsilon$
No.6	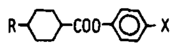	Decrease η and Δn
No.7	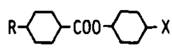	Decrease η and Δn
No.8	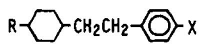	Decrease η
No.9	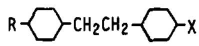	Decrease η and Δn
No.10	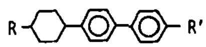	Increase T_{NI} without increase η
No.11	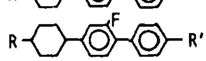	Decrease T_{CN} and increase T_{NI} without increase η
No.12	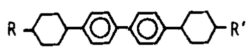	Increase T_{NI}
No.13	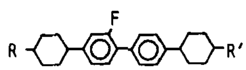	Decrease T_{CN} and increase T_{NI} without increase η
No.14	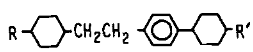	Increase T_{NI} and decrease η and Δn

R, R' : $-C_nH_{2n+1}$ or $-OC_nH_{2n+1}$

X : $-C_nH_{2n+1}$, $-OC_nH_{2n+1}$ or $-CN$

number N as

$$\frac{\overline{V}_{on}}{\overline{V}_{off}} = \frac{\sqrt{\sqrt{N} + 1}}{\sqrt{\sqrt{N} - 1}}$$

The ratio decreases and approaches to 1 as N increases, so that sharp threshold and weak viewing angle-dependency are required for the displays with large number of scanning lines.

The optical properties of the TN-cell is numerically analyzed by Kahn, et al.,[45] Baur, et al.,[46] van Doorn et al.,[47] Nehring, et al.,[48] and others. The general procedure of the analysis is calculating the configuration of director in the liquid crystal layer according to Oseen-Frank elastic theory[49] followed by calculating the transmittance through the liquid crystal layer by Berreman's 4×4 matrix method.[50] According to these theories, material and device parameters which affect the theoretical threshold voltage V_{th}, the optical threshold voltage $V_{10}(\theta)$, threshold sharpness $\rho(\theta)$ and viewing angle dependency $M_{50}(\theta_1, \theta_2)$ are shown in Table VIII, where $V_{10}(\theta)$ denotes voltage which gives 10% change of transmittance from off state at viewing angle of θ from the perpendicular to the cell as shown in Figure 14, $\rho(\theta)$ and $M_{50}(\theta_1, \theta_2)$ are defined as follows,

$$\rho(\theta) = \frac{V_{90}(\theta)}{V_{10}(\theta)}$$

$$M_{50}(\theta_1, \theta_2) = \frac{V_{50}(\theta_1)}{V_{50}(\theta_2)}$$

$V_{90}(\theta)$ and $V_{50}(\theta)$ respectively denote voltages as shown in Figure 14, θ_1 and θ_2 are viewing angles. K_{11} to K_{33} are elastic constants, $\Delta\epsilon$ is dielectric anisotropy, $\epsilon_\perp$ is dielectric constant perpendicular to director, $\Delta n(550)$ is birefringence at wavelength of 550 nm, d is cell gap, and ϕ_0 is pretilt angle. As for Δnd mentioned in Table VIII product of Δn and d must be treated individually in the theory. But in actual, as shown in Figure 15 dependency on individual Δn and d is very weak if Δnd is taken as a parameter.

From the results of numerical calculation, effect of various parameters on the threshold, the threshold sharpness and the viewing angle dependence are summarized as shown in Table VIII,[51] where circle indicates strong dependency. As shown in this table, the threshold voltage $V_{10}(\theta)$ is affected mainly by $\Delta\epsilon$, Δnd and pretilt angle ϕ_0, the

TABLE VIII

Relation between theoretical threshold voltage V_{th}, optical threshold voltage $V_{10}(\theta)$, threshold sharpness $\rho(\theta)$, viewing angle dependency $M_{50}(\theta_1,\theta_2)$ and material and device parameters

	V_{th}	$V_{10}(\theta)$	$\rho(\theta)$	$M_{50}(\theta_1,\theta_2)$
K_{11}	△	△		
K_{22}	△	△		
K_{33}	△	△		
$\Delta\varepsilon$	○	○		
$\varepsilon_\perp$		△		
$\Delta n(550)\cdot d$		○	○	○
ϕ_0	○	○	○	○
K_{33}/K_{11}		△	○	○
K_{33}/K_{22}		△	△	△
$\Delta\varepsilon/\varepsilon_\perp$		○	△	△

○ Strongly depend , △ Weakly depend

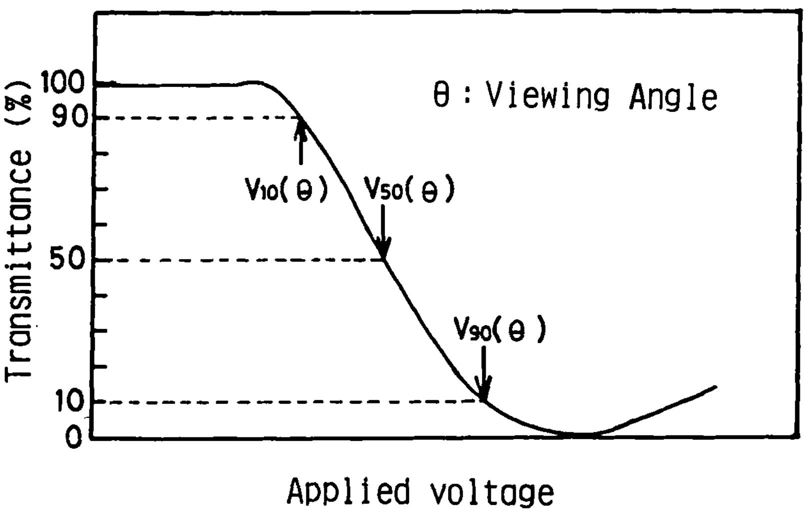

FIGURE 14 Notation of $V_{10}(\theta)$, $V_{50}(\theta)$ and $V_{90}(\theta)$ in the electrooptical property of the TN-cell.

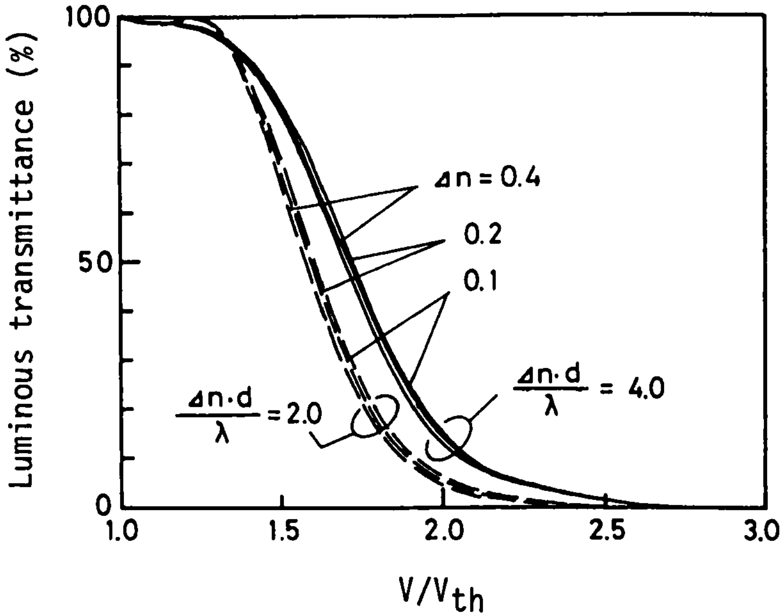

FIGURE 15 The effect of Δn on the electrooptical characteristic of a TN-cell when $\Delta nd/\lambda$ is taken as a parameter.

threshold sharpness depends mainly on ϕ_0 and K_{33}/K_{11}, the viewing angle dependence depends mainly on Δnd, ϕ_0 and K_{33}/K_{11}. Here Δnd is usually adjusted to $1.0 \sim 1.1$ μm for the reason of contrast and interference coloration as mentioned before, and ϕ_0 is about $0.5 \sim 3°$ according to materials of orientation layer and rubbing condition. The effect of ϕ_0 on threshold characteristics are typically as shown in Figure 16, where ordinate is reduced capacitance of the twisted nematic cell and abscissa is reduced applied voltage. The broken lines indicate the range of transmittance between 10% and 90% for various Δnd. From this figure, the shift of the threshold voltage according to the change of ϕ_0 is typically about 2.5%/degree and the change of threshold sharpness is about 1%/degree. Therefore, the difference of ϕ_0 in the range of 0° to 3° can be neglected unless ϕ_0 changes from position to position in the cell.

Considering these background, the most important parameter concerning to the threshold sharpness and the viewing angle dependency is K_{33}/K_{11}, so that many researchers are making effort to synthesize liquid crystal with small K_{33}/K_{11}. Schadt, et al.[52] have measured K_{33}/K_{11} for various types of liquid crystal and their mixture. He reported that

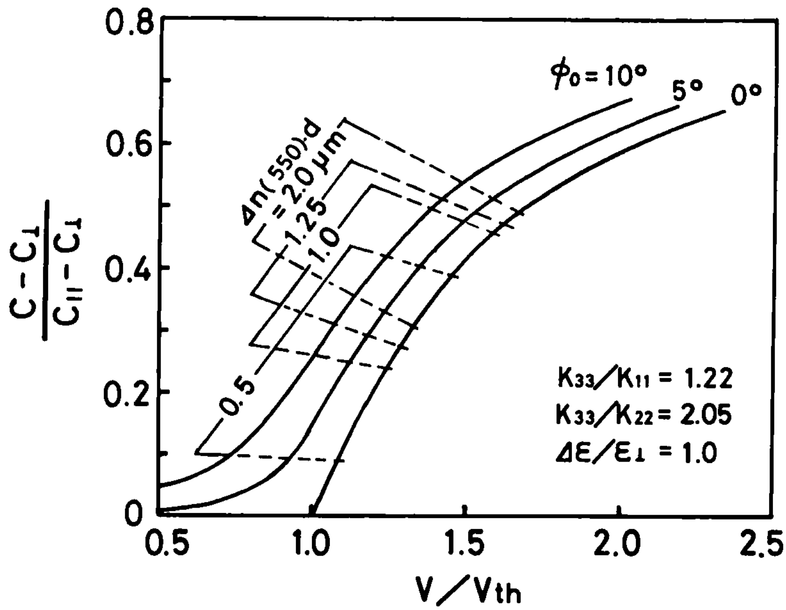

FIGURE 16 Dependence of reduced capacitance of a TN-cell on reduced voltage as a parameter of pretilt angle ϕ_0, where C is capacitance of the cell, the subscripts, $\parallel$ and $\perp$, denote parallel and perpendicular alignments of liquid crystal to electric field, respectively, and V_{th} is the threshold voltage of $\phi_0 = 0$.

pirimidine shown as No. 1 and 3 in Table IX synthesized by his group[53,54] and dioxane shown as No. 4 synthesized by his group,[55] Zaschke, et al.[56] and Sorkin,[57] had small K_{33}/K_{11}. Also, mixtures of No. 3 and 4, and No. 4 and 5 synthesized by Demus, et al.[58] gave fairly small value of K_{33}/K_{11} of about 0.7. Scheuble, et al.[59] has also reported a very small value of 0.5 for No. 2.

By the way, Schadt[52] reported a simplified equation which gives threshold sharpness as a function of K_{33}/K_{11} and $\Delta nd/\lambda$.

$$\frac{V_{50} - V_{10}}{V_{10}} = 0.1330 + 0.0.0266\left(\frac{K_{33}}{K_{11}} - 1\right) + 0.443\left(\ln \frac{\Delta nd}{2\lambda}\right)^2$$

According to this equation, the absolute limit of threshold sharpness ig given by $K_{33}/K_{11} \doteq 0$ and $\Delta nd/2\lambda = 1$. Then, the threshold sharpness becomes 0.11 which corresponds to scanning line number 91. This relation gives a valuable measure of multiplexibility, but it deals with only normal observation. In actual, the high multiplexing liquid crystal display is designed for oblique observation to improve thresh-

TABLE IX

Nematic liquid crystal with small K_{33}/K_{11}

	Liquid Crystal	Reference
No. 1	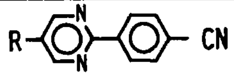	53
No. 2	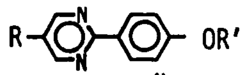	59
No. 3	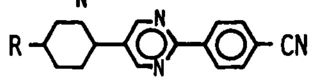	54
No. 4	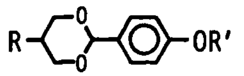	55-57
No. 5	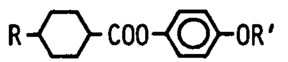	58

old sharpness. In addition, the viewing angle dependence of the threshold within the necessary range of viewing angle must be taken into account.

Therefore, the scanning limitation is actually determined according to the condition as shown in figure 17. This figure shows the schematic transmittance vs. voltage curves for the minimum viewing angle θ_{min} and maximum viewing angle θ_{max}. The limit of the display characteristics is given by the minimum transmittance and minimum contrast ratio in the given range of viewing angle. Therefore, the minimum transmittance T_{min} is given by $T_{off}(L)$, and minimum contrast CR_{min} is given by the ratio of transmittances $T_{off}(H)$ and $T_{on}(H)$. From these conditions, V_{off} and V_{on}, namely the effective voltages applied to on- and off-pixels are determined and which gives the actual limit of the scanning line number. Figure 18 shows the maximum scanning line number calculated for a typical liquid crystal with $K_{33}/K_{11} = 1$ and the other parameters as shown in the figure caption, considering the condition mentioned above. The values in the figures indicates the range of viewing angle. If the minimum acceptable conditions are assumed to be $CR_{min} = 2$, $T_{min} = 60\%$ and the range of viewing angle is between 10° and 30°, the maximum scanning number becomes 65 as shown in Figure 18(a). The maximum line number will be increased up to about 130 by decreasing K_{33}/K_{11}.

For the further increase of the number, adoption of some other method is necessary. One approach to this problem is to use special

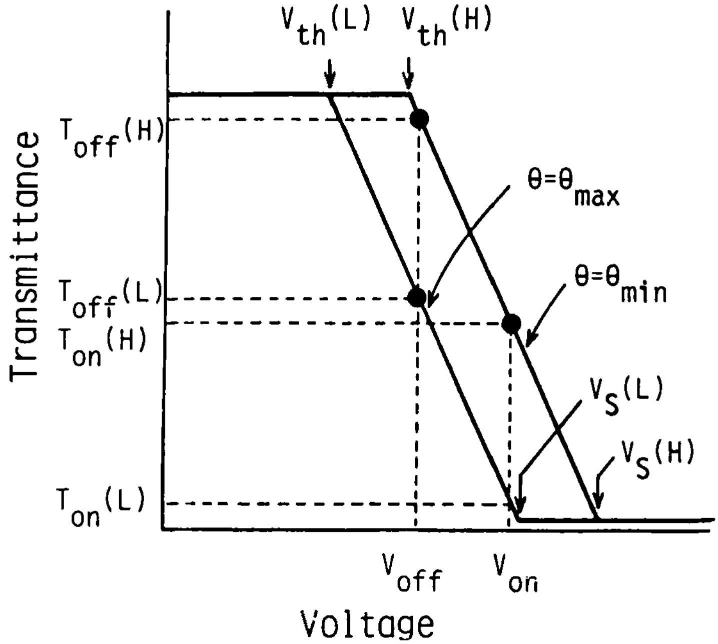

FIGURE 17 Schematic electrooptical characteristics of the TN-cell for two viewing directions, θ_{min} and θ_{max}.

electrode structure or cell structure as shown in Figure 19, which enable to increase the scanning line number without change of duty ratio. Figure (a) shows a devided data electrode structure, which has generally been used in the large scale matrix display. Figure (b) shows a double matrix system in which horizontal electrodes controlling two rows of elements and each element of the double row is connected to a separate column.[60] Figure (c) shows a double electrode layer structure.[61] Figure (d) shows a double liquid crystal layer structure.[62] Combination of these methods is also possible. Problem of these methods is that the number of data electrodes increases according to increase of vertical number of dotes, and hence lead line pitch decreases which requires high technology for lead connection.

Another approach to increase the scanning line number is application of other liquid crystal modes besides the usually addressed TN-mode as follows:

- Electrically controlled birefringent-cell (ECB-cell) with homeotropic alignment.
- Depolarization in a twisted nematic-cell (DTN-cell).

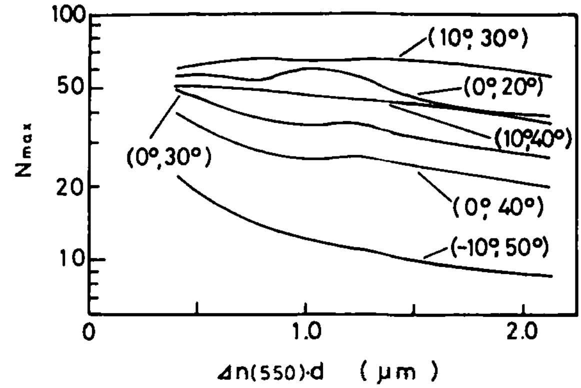

(a) $CR_{min} = 2$, $TR_{min} = 60\%$

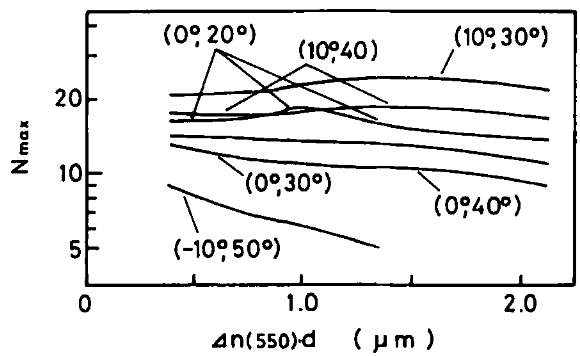

(b) $CR_{min} = 4$, $TR_{min} = 70\%$

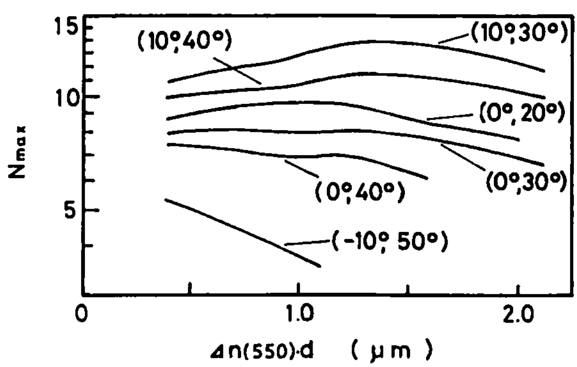

(c) $CR_{min} = 7$, $TR_{min} = 85\%$

FIGURE 18 Maximum number of scanning lines N_{max} of matrix-driving as a function of Δn (550)·d for six different viewing angle ranges and for three different values of CR_{min} and TR_{min} ($K_{33}/K_{11} = 1.0$, $K_{33}/K_{22} = 2.0$, $\Delta\epsilon/\epsilon\perp = 1.0$)

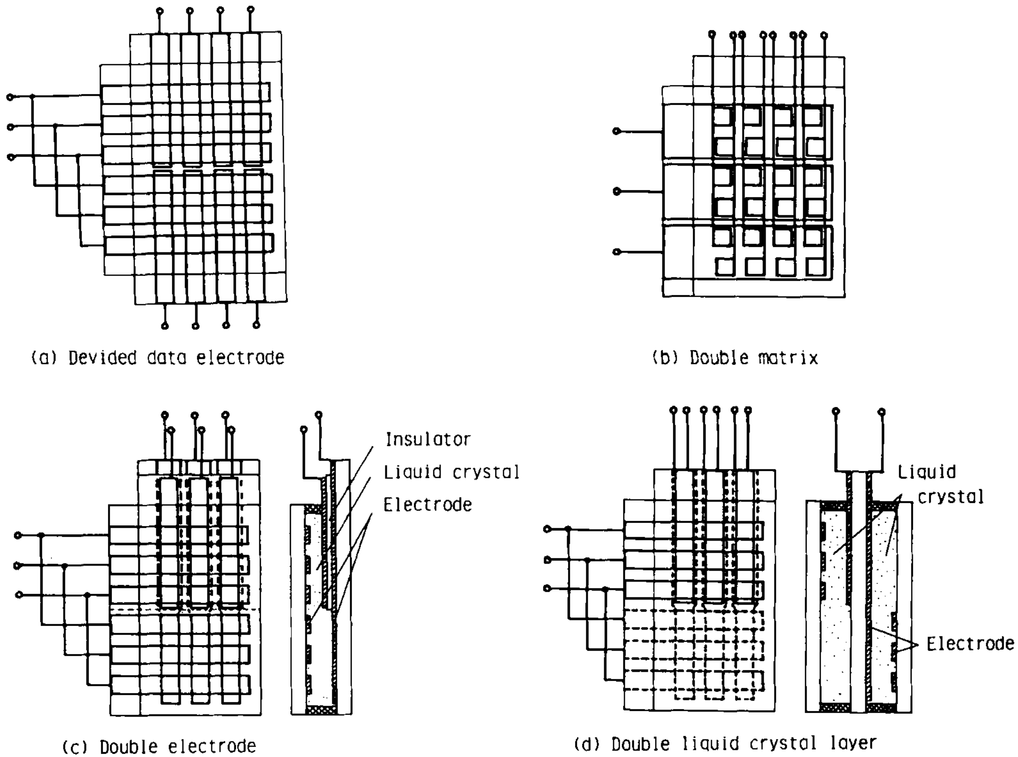

FIGURE 19 Special electrode structure or cell structure of the matrix display for increasing vertical number of pixels without changing duty ratio.

- Two frequency addressing of the TN-cell.
- Thermal addressing of smectic liquid crystal.

The ECB-cell was proposed by Schiekel, et al.,[29] and Assouline, et al.[30] in 1971, and Robert, et al.[63] have developed a matrix display with very large information contents.

The DTN-cell was proposed by the author, et al.[33,34] It has the same structure as the TN-cell except that liquid crystal with negative dielectric anisotropy is used. Advantages of this cell is extremely sharp threshold and very wide viewing angle, while the problem is strong dependency of cut-off frequency[64,65] on temperature.

The two frequency addressing of TN-cell utilizes the change of sign of the dielectric anisotropy with frequency. Dargent, et al.,[66] van Doorn, et al.[67] Hosokawa, et al.[68] and others have reported on this system. Scanning lines can be arbitrary increased but operation voltage increases according to it. Another problem of this system is strong dependency of cross over frequency on temperature.

The thermal addressing of a smectic liquid crystal is proposed by Hareng, et al.[69] and recently Lu, et al.[70] Excellent characteristics are no limit of scanning line number and memory effect. Problems are writing speed and writing power.

5.1.2 Active matrix display

One of the most promising approaches to increase the information contents is active matrix liquid crystal display. Each pixel of this system has an active device, so that it removes from the liquid crystal property the requirement of sharp threshold. The active device used for this system is three terminal switching device as shown in Figure 20(a) or two terminal non-linear device as shown in Figure 20(b).

The three-terminal devices used for this purpose are MOS•FET using single crystal Si wafer reported by Borel et al.,[71] SOS•FET using suphire substrate reported by Lipton et al.[72] and thin film transistor (TFT) using thin film semiconductor on a glass plate reported by Brody, et al.,[73] Fisher, et al.[74] and recently many other researchers. Lately the TFT type has beome of major interest because transparent substrate can be used, which enable the use of the TN-mode with high contrast and have no critical limitation of size. As for the semiconductor material, CdSe was investigated at early times but recently amorphous-Si, poly-Si and laser annealed crystalline-Si is actively investigated.

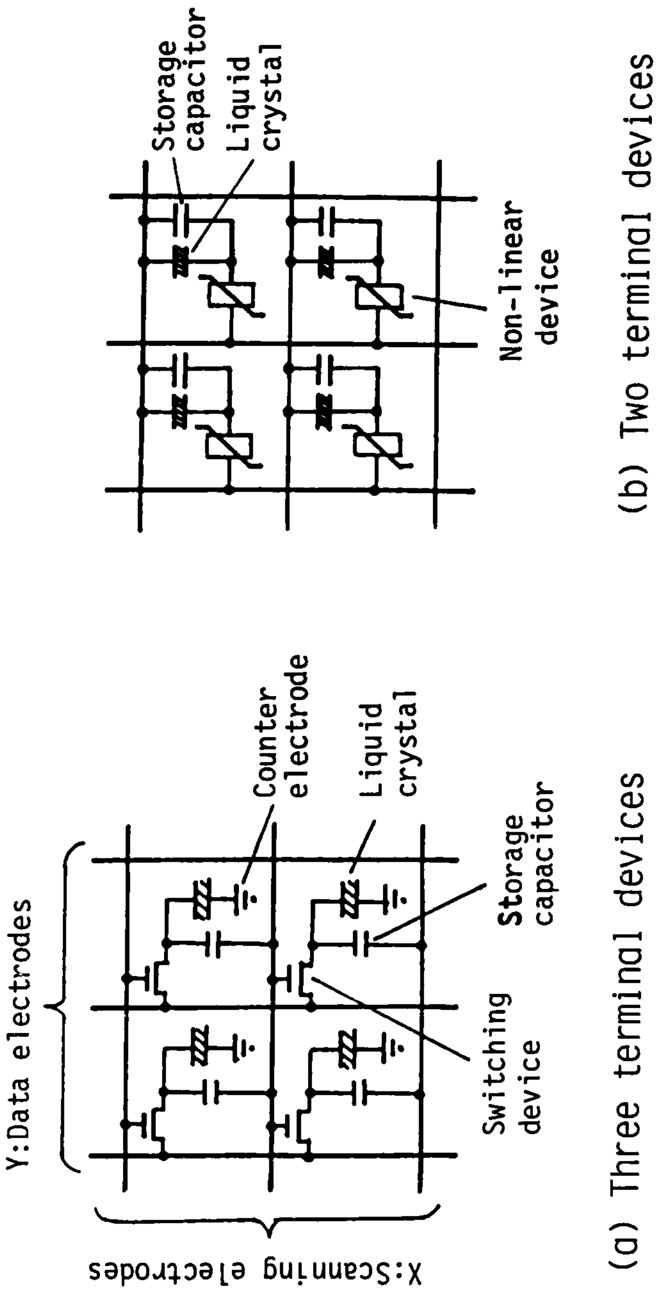

FIGURE 20 Active matrix liquid crystal displays.

On the other hand, the two-terminal devices are varistor reported by Castleberry,[75] metal-insulator-metal (MIM) diode reported by Baraff, et al.[76] back to back diode reported by Szydlo, et al.[77] and diode-ring reported by Togashi, et al.[78]

It has been considered until recently that the two-terminal system is rather difficult to fabricate large scale display because the inhomogeneity of the device properties affects directly to the display property of liquid crystal. But Morozumi, et al.[79] have actually fabricated a large scale matrix display with lateral MIM diodes whose display quality was fairly good. Since then the two terminal devices have attracted interests again. Table X shows remarkable active matrix liquid crystal displays reported recently. Number of dots has attained to 480 X 480 for both MOS•FET type[80] and poly-Si-TFT type,[84] and display area has become 13 X 18 cm for varistor type[85] and 13 cm X 13 cm for amorphous-TFT type.[83] Some of them can display half tone and color image which will be mentioned later.

5.1.3 Laser addressed liquid crystal display

The laser addressing of liquid crystal cell was first reported by Meydan, et al.[87] and Sasaki, et al.[88] Merits of this system are ultra high resolution and memory effect. Dewey, et al.[89] have recently developed a 64 M pel system using smectic liquid crystal.

5.2 Color display

It is agreed upon that a human being is capable of distinguishing about 15 steps of gray shades in a displayed image. But when it comes to the discrimination of hues, the human capability is believed to exceed 200. This suggests that color displays have psychologically more than 13 times as much information content as monochrome displays, although their physical information content is only three times as much.

The feasibility of a multicolor or full-color display was demonstrated early in the emissive flat-panel displays. Nevertheless, they have not been put into practical use as yet because of insufficiency and / or unbalance in luminous efficiency of the various colors. On the other hand, research and development of color liquid crystal displays have progressed rapidly in recent years, and they are fairly close to practical applications.

There seems to be three principles applicable for color liquid crystal

TABLE X

Remarkable active matrix displays reported recently

Type	Material	Laboratory	Number of dots	Active area (cm^2)	LCD mode	Half tone	Color
MOS-FET	Si-wafer	Toshiba[80]	480 X 480	5.3 X 5.3	GH	○	
TFT	CdSe	Xerox[81]	250 X 250	12.7 X 12.7	TN		
TFT	a-Si	Sanyo[82]	220 X 240	4.6 X 6	TN	○	○
TFT	a-Si	Hoshiden[83]	325 X 325	13 X 13	GH		○
TFT	p-Si	Suwa Seiko[84]	480 X 480	6.5 X 8.6	TN	○	○
Varistor	ZnO	G E[85]	180 X 252	13 X 18	GH		
M I M	Ta_2O_5	Suwa Seiko	250 X 240[79]	10 X 9.6	TN		
			220 X 220[86]		TN	○	○
D R*)	a-Si	Citizen[78]	120 X 160		TN	○	

*) Diode rings

displays. Those are interference, dichroism and absorption. Various color liquid crystal displays that operate upon those principles have been proposed as follows:

(1) Interference
  (1a) Electrically controlled birefringent (ECB) cell[23,29,30]
  (1b) Twisted nematic (TN) cells with birefringent films[90]
(2) Dichroism
  (2a) Guest-host (GH) cell
    (i) GH-cell with a polarizer[24]
    (ii) Phase-change type GH-cell[36]
    (iii) Double-layer GH-cell[91]
    (iv) Phase-change type GH-cell with positive image[38]
  (2b) TN-cell with dichroic filter[90,92]
  (2c) Dichroic-mirror type or projection type[93,94]
(3) Absorption: Black-shutter type using a TN-cell or a black GH-cell with color filters or color reflectors.

Among these liquid crystal displays, only the ECB-cell can display multicolor by itself. But unfortunately, the displayed colors are sensitive to change of cell gap, temperature and viewing angle. Therefore, this type of cell required very high technology and is not practically used at present. The other liquid crystal displays besides the ECB-cell are fundamentally monocolor displays.

A multicolor liquid crystal display of the first generation is segment-color display, in which the display area is divided into several parts, and each part has different color filter or dichroic filter. The black-shutter type (3) mentioned above is a typical segment-color display. This type has usually back light. Because of the back light, the display quality of this kind of liquid crystal display became as high as that of emissive displays. Therefore, this kind of display is going to be used to various field in which vivid display is required. In actual, the one using the TN-cell or the double-layer GH-cell has practically been used as automobile display.

On the other hand, multicolor displays capable of displaying changeable color images are realized by using the following principles.

(1) Interference
(2) Subtractive mixing of color components
(3) Additive mixing of color components
  (3a) Mixing of color components projected on a screen
  (3b) Visual mixing of spatially distributed microcolor components.

Here, in the case of interference, the displayed color is limited to the interference color, and therefore full-color is not obtained. While, in the subtractive mixing system and the additive mixing system, full-color can be obtained if the three primary colors of cyan (C), magenta (M), yellow (Y) and the colors red (R), green (G), blue (B), respectively are used for their color components. The mixed color for each system is expressed as follows:
subtractive mixing system:

$$I(\lambda) = I_0(\lambda)\,[T_C(\lambda)]^{K_C}\,[T_M(\lambda)]^{K_M}\,[T_Y(\lambda)]^{K_Y};$$

additive mixing system:

$$I(\lambda) = \alpha I_0(\lambda)\,[K_R T_R(\lambda) + K_G T_G(\lambda) + K_B T_B(\lambda)],$$

where $T_C(\lambda)$, $T_M(\lambda)$, $T_Y(\lambda)$ and $T_R(\lambda)$, $T_G(\lambda)$, $T_B(\lambda)$ are, respectively, spectra corresponding to colors denoted by subscripts. $I_0(\lambda)$ is the luminous spectrum of the light source. K_C, K_M, K_Y and K_R, K_G, K_B denote coefficients of intensity of corresponding colors and are ideally changed between 0 and 1 in the color liquid crystal displays by the applied voltage. α denotes the availability of the incident light. In the case of principles (2) and (3), α is ideally the reciprocal of the color components.

The typical subtractive mixing system is multilayer GH-cell of cyan, magenta and yellow as shown in Figure 21. Figure 22 shows displayed color region of this type that the authors have experimentally fabricated. In this system, a color image is obtained by superposition of two or three primary color images. Therefore, these types have the disadvantage of parallax among images of each color when viewed from an oblique angle. In order to prevent parallax, very thin substrate glass plates or plastic films must be used.

As for the additive mixing system of the projection type (3a), Jacobson, et al.[93] have first realized by using three liquid crystal light valves with photoconductive layer. Another projection type has been realized by Tsai[94] and recently Kubota, et al.[95] by using laser addressed liquid crystal light valves.

The field sequential type (3b) was reported by Clark and Shanks[96] in which a dichroic TN-cell and monochrome CRT was used. Vatne, et al.[97] have replaced the TN-cell with a π-cell to get higher switching speed and wider viewing angle, and have developed color oscilloscopes.

The microcolor components type (3c) has a structure as shown in

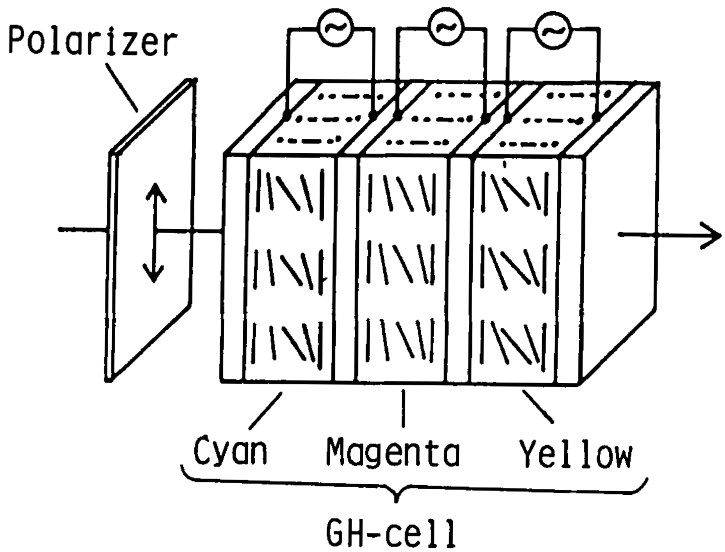

FIGURE 21 A full-color GH-cell with multilayer structure.

Figure 23, where a thin color layers are placed inside the matrix liquid crystal display. This type was proposed and experimentally confirmed by the author, et al.[98,99] and is applicable to both direct matrix and active matrix liquid crystal displays. The primary concept of this type, proposed by Fisher, et al.[100] used mosaic color filters of the three primary colors placed outside of the active matrix liquid crystal display.

Figure 24 shows an example of displayed color image of the cell made by the authors as a trial. The dot size is 95 μm $\times$ 2 mm, the horizontal periodic interval of the same color is 330 μm, and the number of pixels is 432/3 $\times$ 24. Figure 25 shows the displayed color range. Arbitrary color inside the triangle can be displayed by this liquid crystal display. Its color range is quite similar to that of color printed matter, although it is somewhat narrower than that of color CRT.

In Japan, development of this system combined with active matrix has recently become very active. Suwa Seikosha Corporation[101] and Sanyo Electric Corporation[82] have respectively reported pocket color televisions using poly-Si TFT and amorphous-Si TFT with microcolor layer. Hosiden Electronic Corporation[83] has also reported a large color display using a-Si TFT as shown in Table XI.

Disadvantage of this color liquid crystal display is the meager avail-

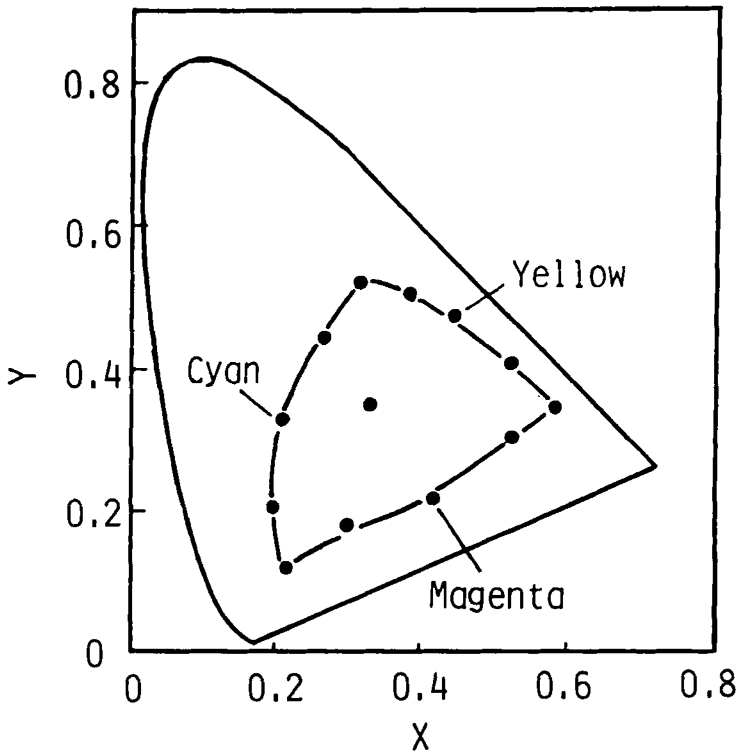

Liquid crystal : GR-41

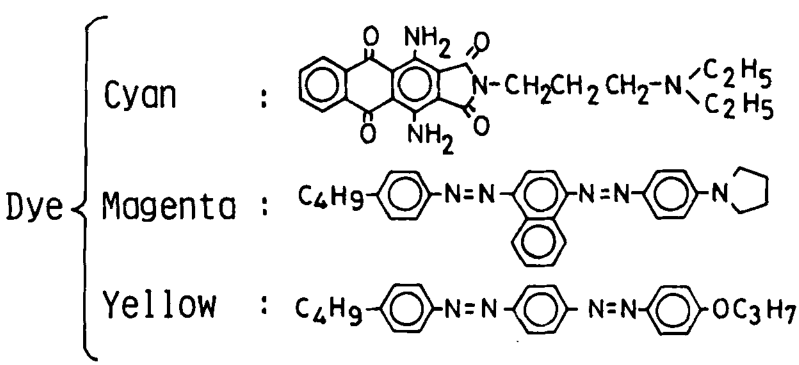

FIGURE 22 A typical example of displayed color range of a multilayer GH-cell on the 1931 CIE chromaticity diagram.

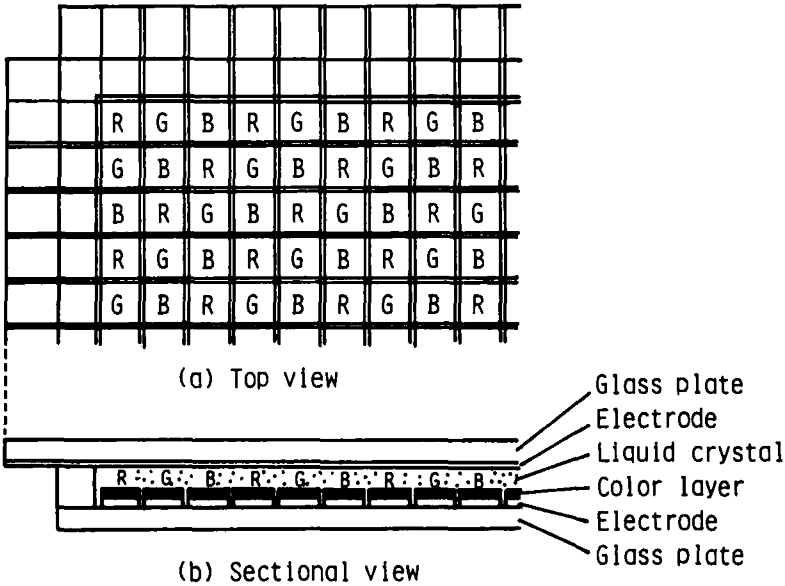

FIGURE 23 Structure of a full-color matrix display with microcolor layers.

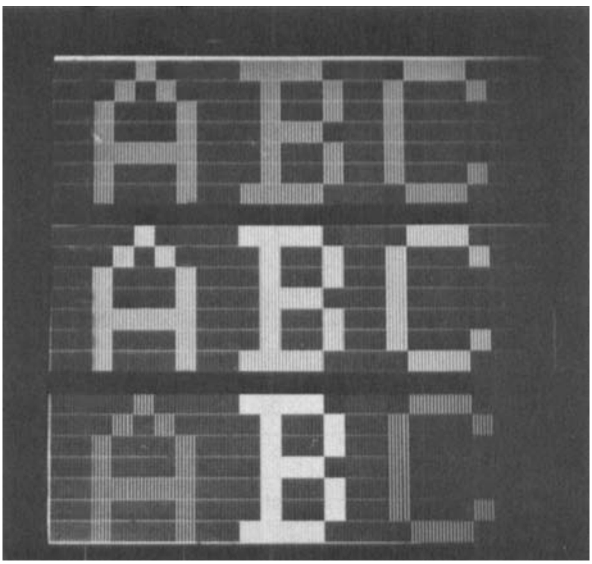

FIGURE 24 An example of displayed characters of violet, red, blue, yellow, purple, green and white on the full-color matrix display.
See Color Plate XI, located in the final volume of these conference proceedings.

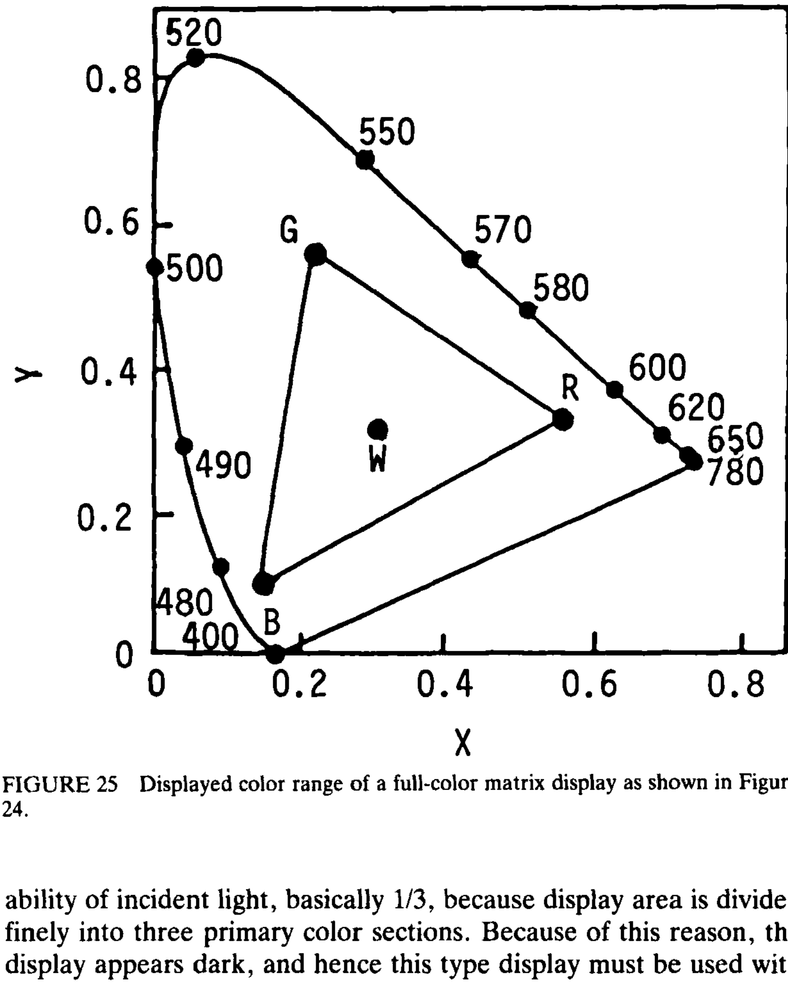

FIGURE 25 Displayed color range of a full-color matrix display as shown in Figure 24.

ability of incident light, basically 1/3, because display area is divided finely into three primary color sections. Because of this reason, the display appears dark, and hence this type display must be used with back light. Therefore, development of a low power back light with high luminous efficiency, preferably with sharp spectra for the primary three colors, and encased within a flat-panel structure is strongly demanded.

5.3 Large screen display

According to expanding of application to automobile displays and large scale matrix displays, size of liquid crystal display increases to about 30 cm diagonal. An important technology on fabrication of large display is cell gap control. Recently, the technique using plastic bease or glass fiber spacer in the active area has been developed and accuracy of the gap of 0.5 to 1 μm is attained.

Still larger displays are also developed. They are projection type and direct-view type. The former is divided into the photo-addressed type using liquid crystal light valves with photoconductive layer and CRTs,[93] and the laser-addressed type.[87–89,94,95] Both of these types have already been mentioned in sections 5.1 and 5.2, so that they are omitted in this section. The direct-view type is composed of liquid crystal display modules, and hence the size and number of pixels are arbitrary designed by choosing number of modules. Myodo, et al.[102] and Takada, et al.[103] have recently developed full-color television display of this type (see Table XI), in which the TN-mode and the black GH-mode are respectively used, and three primary micro-color layers are placed outside of the cells. Their typical size is 1.7 m to 5.4 m in diagonal. They are promising as a large screen flat panel display.

5.4 Improvement of switching speed

As long as application to display devices, required switching time is about 20 msec. The usual response time of the static driven TN-cell is just around these values, but it increases in the halftone display or high multiplexing display. Therefore, roughly speaking, about one order faster response than present device is desired.

In order to improve the response speed, several methods have been proposed. The triode gate structure for applying lateral electric field is proposed by Channin and Carlson.[104] The two frequency driving of the TN-cell are proposed by Baur, et al.,[105] Raynes, et al.[106] and other researchers. A π-cell is proposed by Vatne, et al.[97] While, these method is useful mainly for decreasing the recovery time up to about 1 order. On the other hand, Clark, et al.[107] reported submicrosecond bistable electro-optic switching in a chiral smectic C liquid crystal cell. Since then, this liquid crystal has attracted many interests. While, there are several practical problems at present such as requirements of very narrow cell gap of 1 to 2 μm and homogeneous alignment of weak azimuth anchoring.

6. SUMMARY

Application of liquid crystal display started in small numeric displays, but its information contents has been increasing year by year, and direct matrix liquid crystal displays is going to approach to the level of low resolution CRTs, and active matrix displays to middle reso-

TABLE XI

Most recent remarkable liquid crystal displays and their characteristics compared with the CRT

	Type	Laboratory	Number of dots	Active area (cm)	Information contents	Size	Resolution	Color	Video display	Flatness
(1)	Direct matrix		~200 X 640	~10 X 30	○	△	△	△	△	◎
(2)	Active matrix (MOS-FET)	Toshiba[80]	480 X 480	5.3 X 5.3	○	△	○			
(3)	do (p-Si-TFT)	Suwa Seikosha[84]	480 X 480	8.6 X 6.5	○	△	○	○	○	◎
(4)	do (a-Si-TFT)	Hoshiden[83]	325 X 325	13 X 13	○	△	△	○		◎
(5)	do (Varistor)	G E[85]	180 X 252	13 X 18	△	△	△			◎
(6)	do (M I M)	Suwa Seikosha[79,86]	250 X 240	10 X 9.6	△	△	△	○	△	◎
(7)	Thermally addressed LCD	Kylex[70]	512 X 576	15.2 X 17.8	○	△	△			◎
(8)	Laser addressed LCD	I B M[89]	8000 X 8000	10 X 10	◎	◎*	◎			×
(9)	do	Singer[94]	2048 X 2048	2.5 X 2.5	◎	◎*	◎	△		×
(10)	Light addressed LCD	Hughes[93]	600 line	5.1φ	○	◎*	○	○	○	×
(11)	Direct view - large screen	Mitsubishi[102] Matsushita[103]	~400 X 640	~2.9 X 4.6 m	○	◎	△	○	○	◎

* Projection type

lution CRTs. In addition, by comparison with the other emissive flat panel display, the information contents of the liquid crystal displays are inferior to plasma displays but comparable to vacuum fluorescent displays and electro luminescent displays. In the view point of the full-color display, the liquid crystal displays have made such progress that it can be put to practical use.

Table XI shows the most recent remarkable liquid crystal displays made as a trial, where characteristics of them are compared with those of the CRTs. Double circle indicates that the liquid crystal display surpasses the CRT in the concerning item, circle indicates comparable, triangle a little inferior and crossed symbol clearly inferior. As shown in this table, for the small size and very large size, the liquid crystal display has already overcome the CRT. The most difficult size for the liquid crystal display with high information contents is 30 ~ 50 cm in diagonal. Development of this size is a subject for a future study.

In any way, the progress of the electronics, especially semiconductor electronics directs micro-technology which requires low voltage and low current devices. In this point of view, the liquid crystal display is most promising among various devices.

Acknowledgment

The author would like to express his hearty thanks to Prof. Yukio Shibata for his valuable discussion and to Dr. Hidehiro Seki and Mr. Masanobu Onodera for their assistance.

References

1. J. L. Fergason: *Sci. AM.*, **211**, 77 (1964).
2. G. H. Heilmeier, L. A. Zanoni and L. A. Barton: *Proc. IEEE*, **56**, 1162 (1968).
3. L. T. Creagh and A. R. Kmetz: *Mol. Cryst. Liq. Cryst.*, **24**, 59 (1973).
4. F. J. Kahn, G. N. Taylor and H. Schonhorn: *Proc. IEEE*, **61**, 823 (1973).
5. G. Porte: *J. Phys.*, **37**, 1245 (1976).
6. I. Haller: *Appl. Phys. Lett.*, **24**, 349 (1974).
7. T. Uchida, K. Ishikawa and M. Wada: *Mol. Cryst. Liq. Cryst.*, **60**, 37 (1980).
8. M. Ohgawara, T. Uchida and M. Wada: *Mol. Cryst. Liq. Cryst.*, **74**, 227 (1981).
9. T. Uchida, M. Ohgawara and Y. Shibata: *Mol. Cryst. Liq. Cryst.*, **98**, 146 (1983).
10. I. Haller: *J. Chem. Phys.*, **57**, 1400 (1972).
11. W. Helfrich: *Phys. Lett.*, **35A**, 393 (1971).
12. J. E. Proust, L. Ter-Minassian-Saraga and E. Guyon: *Solid State Commun.*, **11**, 1227 (1972).
13. T. Uchida, C. Shishido and M. Wada: *Electro. Commun. Japan*, **58-C**, 132 (1975).
14. M. Kawachi, O. Kogure and Y. Kato: *Japan. J. Appl. Phys.*, **13**, 1457 (1974).
15. K. Hiroshima: *Japan. J. Appl. Phys.*, **21**, L791 (1982).

16. F. Funada, H. Uede, T. Wada and S. Mito: *Proc. of the 1st Japanese Liquid Crystal Conference*, p.45 (1975), (in Japanese).
17. J. C. Dubois, M. Gazard and A. Zann: *J. Appl. Phys.*, **47**, 1270 (1976).
18. T. Uchida, M. Takeda and M. Wada: *Proc. of the 5th Japanese Liquid Crystal Conference*, p.36 (1979), (in Japanese).
19. D. W. Berreman: *Phys. Rev. Lett.*, **28**, 1683 (1972).
20. J. L. Janning: *Appl. Phys. Lett.*, **21**, 173 (1972).
21. L. A. Goodman, J. T. Mcginn, C. H. Anderson and F. Digeronimo: *IEEE Trans.*, **ED-24**, 795 (1977).
22. T. Uchida, M. Ohgawara and M. Wada: *Japan. J. Appl. Phys.*, **19**, 2127 (1980).
23. H. Gruler and G. Meier: *Mol. Cryst. Liq. Cryst.*, **16**, 299 (1972).
24. G. H. Heilmeier and L. A. Zanoni: *Appl. Phys. Lett.*, **13**, 91 (1968).
25. T. Shimomura, H. Mada, K. Uehara, S. K. Min and S. Kobayashi: *Japan. J. Appl. Phys.*, **14**, 1093 (1975).
26. M. Schadt and W. Helfrich: *Appl. Phys. Lett.*, **18**, 127 (1971).
27. T. Uchida, H. Seki, C. Shishido and M. Wada: *Mol. Cryst. Liq. Cryst.*, **54**, 161 (1979).
28. S. Matsumoto, M. Kawamoto and K. Mizunoya: *J. Appl. Phys.*, **47**, 3842 (1976).
29. M. F. Schiekel and K. Fahrenschon: *Appl. Phys. Lett.*, **19**, 391 (1971).
30. G. Assouline, M. Hareng and E. Leiba: *Elec. Lett.*, **7**, 699 (1971).
31. T. Uchida, H. Seki, C. Shishido and M. Wada: *IEEE Trans.*, **ED-26**, 1373 (1976); *Mol. Cryst. Liq. Cryst.*, **54**, 161 (1979).
32. M. Kuwahara, H. Onnagawa and K. Miyashita: *Proc. of the 1st Japanese Liquid Crystal Conference*, p.43 (1975), (in Japanese).
33. T. Uchida, Y. Ishii and M. Wada: *IEEE Trans.*, **ED-26**, 1375 (1979). *Proc. SID*, **21**, 55 (1980).
34. I. Fukuda, M. Akatsuka, T. Uchida and M. Wada: *Mol. Cryst. Liq. Cryst.*, **68**, 311 (1981).
35. J. J. Wysocki, A. Adams and W. Haas: *Phys. Rev. Lett.*, **20**, 1024 (1968).
36. D. L. White and G. N. Taylor: *J. Appl. Phys.*, **45**, 4718 (1974).
37. T. Uchida, C. Shishido and M. Wada: *Elec. Commun. Japan*, **57-C**, 103 (1974).
38. F. Gharadjedaghi: *The 8th Int'l Liquid Crystal Conf.*, I-32P (1980).
39. W. Haas, J. Adams, and J. B. Flannery: *Phys. Rev. Lett.*, **24**, 577 (1970).
40. C. H. Gooch and H. A. Tarry: *J. Phys.*, **D, 8**, 1575 (1975).
41. F. Gharadjedaghi and J. Robert: *J. Phys. Appl.*, **10**, 69 (1975).
42. L. Pohl, G. Weber, R. Eidenschink, G. Baur and W. Fehrenback: *Appl. Phys. Lett.*, **38**, 497 (1981).
43. G. W. Gray, K. J. Harrison and J. A. Nash: *Elec. Lett.*, **9**, 130 (1973).
44. P. M. Alt and P. Pleshko: *IEEE Trans.*, **ED-21**, 146 (1974).
45. F. J. Kahn and H. Birecki: "The Physics and Chemistry of Liquid Crystal Devices," p.79, edited by G. J. Sprokel, Plenum Press, New York/London, 1980.
46. G. Baur: "The Physics and Chemistry of Liquid Crystal Devices," p.61, edited by G. J. Sprokel, Plenum Press, New York/London, 1980: *Mol. Cryst. Liq. Cryst.*, **63**, 45 (1981).
47. C. Z. van Doorn, C. J. Gerritsma and J. J. M. J. de Klerk: "The Physics and Chemistry of Liquid Crystal Devices," p.95, edited by G. J. Sprokel, Plenum Press, New York/London, 1980.
48. J. Nehring: "Advances in Liquid Crystal Research and Applications," p.1155, edited by Lajos Bata, Pergamon Press, Oxford, 1980.
49. F. C. Frank: *Disc. Faraday Soc.*, **25**, 19 (1958).
50. D. W. Berreman: *J. Opt. Soc. Am.*, **62**, 502 (1972): *J. Opt. Soc. Am.*, **63**, 1374 (1973).
51. Y. Takahashi and T. Uchida: *Papers of Technical Group on Electron Devices, I.E.C.E. Japan,* ED80-80, 13, (1980), (in Japanese).
52. M. Schadt and P. R. Gerber: *Z. Naturforsch.* **37a**, 165 (1982).
53. A. Boller, M. Cereghetti, M. Schadt and H. Scherrer: *Mol. Cryst. Liq. Cryst.*, **42**, 215 (1977).

54. A. Villiger, A. Boller and M. Schadt: *Z. Naturforsch*, **34b**, 1535 (1979).
55. A. Boller, A. Germann, M. Schadt and A. Villiger: Swiss Patent Application Nr. 10154/79 (1979).
56. H. Zaschke, H. M. Vorbroth, D. Demus and H. Kresse: GOR Patent Nr.139867 (1978).
57. H. Sorkin: *Mol. Cryst. Liq. Cryst.*, **57**, (Lett.), 279 (1980).
58. D. Demus, H. J. Deutscher, F. Kuschel and H. Schubert: German Patent Nr.2429093 (1973).
59. B. S. Scheuble and G. Baur: *Proc. Japan Display*, 224 (1983).
60. E. Kaneko, H. Kawakami and H. Hanmura: *SID Symp. Digest*, 92 (1978).
61. T. Kamikawa: *SID Symp. Digest*, 196 (1980).
62. S. Yasuda, T. Takamatsu, S. Kozaki, S. Minezaki and T. Wada: *The 8th Int'l Liq. Cryst. Conf.*, I-21P (1980).
63. J. Robert and F. Clerc: *SID Symp. Digest*, 30 (1980).
64. E. D. Violette, P. G. de Gennes and O. Parodi: *J. Phys.*, **32**, 305 (1971).
65. Orsay Liquid Crystal Group: *Mol. Cryst. Liq. Cryst.*, **12**, 251 (1971).
66. B. Dargent and J. Robert: *SID Symp. Digest*, 60 (1977).
67. C. Z. van Doorn and J. de Klerk: *SID Symp. Digest*, 100 (1978).
68. M. Hosokawa, S. Kanbe, M. Nagata and H. Nakamura: *SID Symp. Digest*, 116 (1979).
69. M. Hareng, S. L. Berre, R. Hehlen and J. N. Perbet: *SID Symp. Digest*, 106 (1981).
70. S. Lu, D. H. Davies, C. H. Chung, D. Evanicky, R. Albert and T. Traber: *Record of Int'l Display Res. Conf.*, 132 (1982).
71. J. Borel: *SID Symp. Digest*, 128 (1971).
72. L. T. Lipton, M. A. Meyer and D. O. Massetti: *SID Symp. Digest*, 78 (1975).
73. T. P. Brody, J. A. Asars and G. D. Dixon: *IEEE Trans.*, **ED-20**, 995 (1973).
74. A. G. Fischer: *IEEE Trans.*, **ED-18**, 802 (1971).
75. D. E. Castleberry: *IEEE Trans.*, **ED-26**, 1123 (1979).
76. D. R. Baraff, J. R. Long, B. K. MacLaurin, C. J. Miner and R. W. Streater: *IEEE Trans.*, **ED-28**, 736 (1981).
77. N. Szydlo, E. Chartier, J. N. Perbert, N. Proust, J. Magarinor and M. Hareng: *Proc. Japan Display*, 416 (1983).
78. S. Togashi, K. Sekiguchi, H. Tanabe, E. Yamamoto, K. Sorimachi, E. Tajima, H. Watanabe and H. Shimizu: *SID Symp. Digest*, 324 (1984).
79. S. Morozumi, T. Ohta, R. Araki, T. Sonehara, K. Kubota, Y. Ono, T. Nakagawa and H. Ohara: *Proc. Japan Display*, 404 (1983).
80. K. Kasahara, K. Sakai, Y. Komatsubara, A. Saito, K. Ide, S. Matsumoto and H. Hori: *SID Symp. Digest*, 150 (1983).
81. F. C. Luo and D. Hoesly: *SID Symp. Digest*, 46 (1982).
82. M. Yamano, H. Ikeda, H. Takesada, M. Yamasaki, Y. Okita, S. Sugibuchi and Y. Sasaki: *Proc. Japan Display*, 44 (1983).
83. Y. Ugai, Y. Murakami, J. Tamamura and S. Aoki: *SID Symp. Digest*, 308 (1984).
84. S. Morozumi, K. Oguchi, T. Misawa, R. Araki and H. Ohshima: *SID Symp. Digest*, 316 (1984).
85. D. E. Castleberry, C. A. Becker and L. M. Levinson: *SID Symp. Digest*, 264 (1982).
86. K. Niwa, S. Maezawa, M. Suzuki, T. Takeuchi and T. Kamikawa: *SID Symp. Digest*, 304 (1984).
87. D. Maydan, H. Melchior and F. Kahn: *IEEE Conf. Record of 1972 Conf. on Display Devices*, 166 (1972).
88. A. Sasaki, K. Kurahashi and T. Takagi: *IEEE Conf. Record of 1972 Conf. on Display Devices*, 161 (1972).
89. A. G. Dewey, S. F. Anderson, G. Cheroff, J. S. Feng, C. Handen, H. W. Johnson, J. Leff, R. T. Lynch, C. Marinelli and R. W. Schmiedeskamp: *SID Symp. Digest*, 36 (1983).

90. T. J. Scheffer: *J. Appl. Phys.*, **44**, 4799 (1973).
91. T. Uchida, H. Seki, C. Shishido and M. Wada: *Proc. SID*, **22**, 41 (1981).
92. S. Kobayashi and F. Takeuchi: *SID Symp. Digest*, 40 (1973).
93. A. D. Jacobson, D. D. Boswell, J. Grinberg, W. P. Bleha, P. G. Reif, B. Hong, S. G. Lundquist and J. H. Colks: *SID Symp. Digest*, 106 (1977).
94. R. C. Tsai: *Information Display*, 3 (May 1981).
95. K. Kubota, S. Sugama, S. Naemura and N. Nishida: *SID Symp. Digest*, 44 (1983).
96. M. G. Clark and I. A. Shanks: *SID Symp. Digest*, 172 (1982).
97. R. Vatne, P. A. Johnson, Jr. and P. J. Bos: *SID Symp Digest*, 28 (1983).
98. T. Uchida: *Proc. Eurodisplay*, 39 (1981).
99. T. Uchida, S. Yamamoto and Y. Shibata: *IEEE Trans.*, **ED-30**, 503 (1983).
100. A. G. Fisher, T. P. Brody and W. S. Escott: *IEEE Conf. Record on Display Devices*, 64 (1972).
101. S. Morozumi, K. Oguchi, S. Yazawa, T. Kodaira, H. Ohshima and T. Mano: *SID Symp. Digest*, 156 (1983).
102. O. Myodo, K. Yagishita, M. Ohta and K. Kurahashi: *Proc. Japan Display*, 210 (1983).
103. A. Takada, T. Ohashi and Y. Wakahata: *Meeting of Community 142 of the Japan Society for the Promotion of Science* (Nov. 1983).
104. D. J. Channin and D. E. Carlson: *Appl. Phys. Lett.*, **28**, 300 (1976).
105. G. Baur, A. Stieb and G. Meier: *Appl. Phys.* **2**, 349 (1973).
106. E. P. Raynes and I. A. Shanks: *Elec. Lett.*, **10**, 114 (1974).
107. N. A. Clark and S. T. Lagerwall: *Appl. Phys. Lett.*, **36**, 899 (1980).